Hub connectivity in the human connectome: Links to aging and processing speed

Xin Li[1]*, Alireza Salami[1,2,3], and Jonas Persson[1,4]

[1]Aging Research Center, Karolinska Institute and Stockholm University, Stockholm, Sweden

[2]Umeå Center for Functional Brain Imaging (UFBI), Umeå University, Umeå, Sweden.

[3]Wallenberg Centre for Molecular Medicine, Umeå University, Umeå, Sweden.

[4]Center for Lifespan Developmental Research (LEADER), School of Law, Psychology and Social Work, Örebro University, Örebro, Sweden

Abstract

The human structural brain network, or connectome, has a rich-club organization with a small number of brain regions showing high network connectivity, called hubs. Hubs are centrally located in the network, biological costly, and might be critical for human cognition. Normal aging is accompanied by cognitive decline, including processing speed, and has been linked to energy depletion in the neurons at a molecular level. However, it is still unclear how age affects hub connections in human connectome. Using a large healthy sample (N=137) with wide age range (25-85 years), we found that the anatomical locations of hubs are relatively age-invariant. However, there were wide-spread age effects on the connectivity strength in the connectome. Critically, these age effects were larger in connections within hubs compared to more peripheral brain regions. These findings were supported by both cross-sectional and longitudinal (N=83) analyses. Moreover, results demonstrated associations between connectivity strength and processing speed, which were more concentrated in hub connections than chance level, and the connectivity strength in hub connections mediated the age-effects on processing speed. Overall, our findings indicate that the hub connections are especially affected by aging, and their vulnerability to the age effects might explain the lower processing speed in older adults.

Introduction

The human brain can be viewed as a network at the macroscopic level, with individual brain regions, nodes, interconnected by white matter (WM) fibers. Accumulating evidence suggest a brain organization with the topological properties of a complex scale-free network (Power et al., 2013; van den Heuvel and Sporns, 2011). A scale-free network is characterized by the probability of nodes degree (i.e., the number of connections to other nodes) in the network decaying as a power law, free of a characteristic scale, for large degrees. A scale-free network indicate the existence of a subset of nodes having a large proportion of connections in the network. Brain network connectivity is highly

heterogeneous, and has a long-tailed distribution of nodes degree, indicating that a subset of nodes are more highly connected than other nodes (Achard and Bullmore, 2007; Eguíluz et al., 2005; Sporns et al., 2007; van den Heuvel and Sporns, 2013).

The highly connected nodes in a brain network are called "brain hubs". The spatial distance among hubs is relatively longer compared to the distance among peripheral nodes (Alexander-Bloch et al., 2013; Van Den Heuvel et al., 2012). This indicates that brain hubs have high anatomical wiring cost and are critical for integrating brain sub-networks and transforming information among long-distance brain regions. In addition, hubs, especially in the cortical area, have proportionally greater metabolic rate (Liang et al., 2013; Tomasi et al., 2013; Vaishnavi et al., 2010), suggesting that maintaining normal function of hubs is energy costly. Hubs are also disproportionately expanded in humans than other primates (Hill et al., 2010). Thus, the existence of hubs might partly explain cognitive capabilities in humans (Buckner and Krienen, 2013). Brain lesions linked to various brain disorders, including schizophrenia and Alzheimer's disease, are disproportionately concentrated in brain hubs compared to more peripheral brain regions (Buckner et al., 2009; Crossley et al., 2014). Possibly, the high metabolic cost and long-distance connections of hubs make them vulnerable to pathological damage, such as shortage of metabolic energy supply or oxidative stress.

Aging is associated with changes in brain structure and function, as well as with cognitive decline. Both cross-sectional and longitudinal studies have demonstrated effects of age on WM micro-/macro-structures. These studies typically include measures of fractional anisotropy (FA) and mean diffusivity (MD) based on tensor model in diffusion tensor imaging (DTI), but also on estimates of WM fiber density (FD) and cross-section (FC) based on constrained spherical deconvolution (CSD) model of WM fiber function. At the network level, a recent longitudinal study demonstrated structural connectome reorganization as indicated by both decreased integration and increased segregation, reflecting more differentiation of structural organization over a mean of 5-years follow-up (Coelho et al., 2021). This pattern is in contrast with age-related dedifferentiation of the brain networks derived from cortical thickness (Chen et al., 2011) and functional connectivity (e.g., Chan et al., 2014; Pedersen et al., 2021), and the underlying reason for structural changes is unknown.

No study to date has investigated changes in hubs in normal adults. A handful of studies have found that multiple topological properties, such as global network efficiency and connectivity strength, is lower in older age, particularly after the age of 60 (Gong et al., 2009; Zhao et al., 2015). Computational work has also shown that when hubs in a brain network were attacked by modeled pathological damage, global efficiency deteriorated more rapidly compared to when nodes were targeted randomly (Crossley et al., 2014). Thus, it is possible that the effect of advancing age on network efficiency is driven by greater reduced structural connectivity strength within hubs compared to more peripheral regions. At a molecular level, it has been proposed that the normal aging process

is characterized by a progressive accumulation of damage induced by reactive oxygen, nitrogen, and carbonyl species (RONCS). RONCS is the by-products of various catabolic and anabolic processes that can cause oxidative deterioration of DNA, protein, and lipid. This can lead to subsequent energy depletion in the cell and cause cell death. Based on this chain of events, one might hypothesize that hub regions and long-distance hub-hub connections are more likely to be affected by decreased energy metabolism induced by the oxidative damage associated with normal aging. There is no study has systematically examined if connections within hubs are more effected by age than peripheral regions in structural networks. To address these questions, the current study aims to investigate the age effects on structural hubs using both cross-sectional data with wide age range from 25-85 years and longitudinal data with five-year interval.

Moreover, a previous DTI study has shown that age-related differences in WM integrity can partly explain the age-differences in tasks that require speeded responses (Andersson et al., 2022; Li et al., 2022; Salami et al., 2012). Indeed, processing speed has been highly correlated with higher-order cognition, such as working memory and fluid intelligence (Ackerman et al., 2002; Waters and Caplan, 2005), and has been suggested as an underlying cause of accelerated cognitive impairment across task domains in older adults (Finkel et al., 2005). It is currently unknown whether hub-hub connections are more critical for cognitive performance, such as processing speed, compared to peripheral connections in older adults.

In this study, we investigate the age effects on human structural hubs and its relation with processing speed using both edge-wise network-based analysis and a graph-theoretical approach (Figure 1). It should be noted that the distinction between hubs and non-hubs, especially for a brain network, is relatively arbitrary. Except defining hubs using degree centrality, previous studies also used cluster coefficiency, betweenness centrality, shortest path, or a combined score of several measures to define how a brain region is central/influential in a network. Moreover, there is no consensus on the cut-off for distinguishing hubs from non-hubs. To overcome this issue, the current study used both degree and a combined measure of centrality to define hubs (Van Den Heuvel et al., 2010). Also, our graph-theoretical analysis was conducted on multiple varying thresholds instead of using a hard cut-off to define hubs. We hypothesize that, (1) the *locations* of hubs in a structural brain network remain stable across the adults life span, but that (2) there are wide-spread age effects on *connectivity strength* across the connectome; more importantly (3) the age effects on connectivity strength are larger within hubs compared to peripheral connections; and finally that (4) the connectivity strength in hub connections are more strongly related to processing speed compared to peripheral connections, such that connections of high-degree nodes can explain processing speed impairments in older adults.

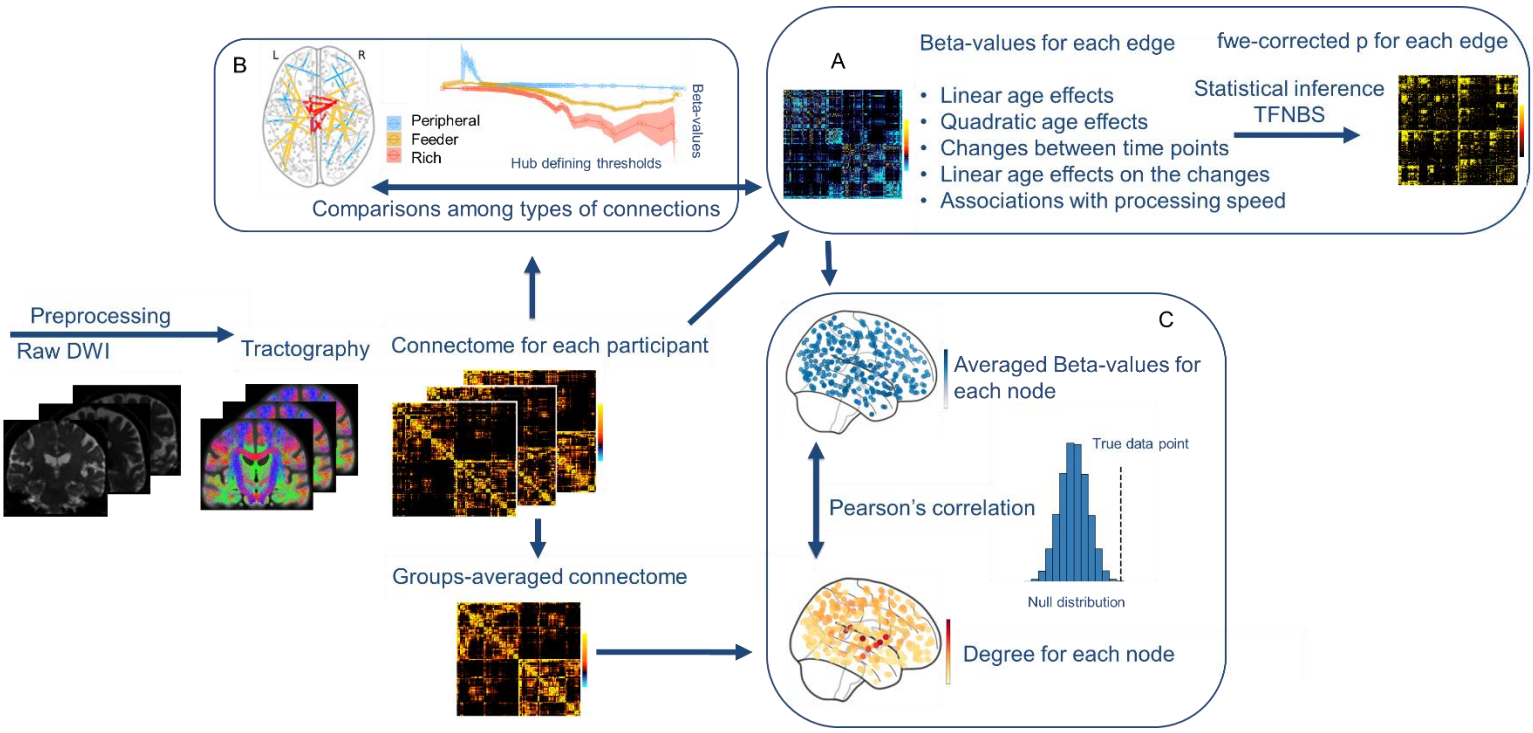

Figure 1. Schematic illustration of the pipeline. After preprocessing, (A) connectivity strength in the connectome was associated with age or speed using regression. Threshold-free network-based analysis (TFNBS) was applied to estimate the beta- and p- values for each edge. (B) Degree/hubness of each node was derived from the connectome using graph theory. Rich/feeder/peripheral connections were defined based on multiple thresholds of degree/hubness. The beta-values of each edge were compared among rich/feeder/peripheral connections. (C) Beta-values were averaged for each nodes, which were than correlated with the map of degree of each nodes.

Methods

1. Participants

The participants in the current study are part of the Betula prospective cohort study on memory, health and aging (Nilsson et al., 1997; Nyberg et al., 2020). The Betula study was approved by the Regional Ethical Review Board in Umeå, and all participants gave written informed consent. The Betula project was launched in 1988 and 7 waves of health and neuropsychology data until 2017 (T1-T7) have been collected. The time interval between the waves is five years. The current study is based on the neuroimaging subsample recruited from the T5 to T7 waves. The original sample size of the 3 waves is 376 (T5), 230 (T6), and 103 (T7). We excluded participants with dementia, stroke, epilepsy, Parkinson's disease, multiple sclerosis, hydrocephalus, head surgery, deviant brain morphology, vascular brain lesions and infarcts. Dementia was assessed at baseline and reassessed for each wave

using a three-step procedure, according to the Diagnostic and Statistical Manual of Mental Disorders, 4th edition (DSM–IV; American Psychiatric Association, 1994). First, an overall evaluation was performed by an examining physician. The diagnosis was then compared with a second independent diagnosis based on scores from several cognitive tests. In cases of disagreement, a supervising physician made a third and final diagnosis. Cross-sectional analysis was conducted on the data of wave T5, which has the largest sample size. In the age-comparison analyses, five age groups: 25-45, 50-55, 60-65, 70-75 and 80-85 years were defined and compared.

In this sample, echo time (TE) varies within waves, and between T5 and T6/T7 waves. Since TE may potentially influence the estimated WM fiber densities, longitudinal analyses were carried out for T6 and T7 only. Participants with different TEs at T5 and with changes of TE between T6 and T7 were excluded. The demographic information and behavioral performance of processing speed of the final sample are present in Table 1.

Table 1 Demographic information and cognitive performance

	T5	T6	T7
	Cross-sectional design	Longitudinal design	
N	137	84	
Age	62 (25-85)	69.2 (55-80) at T6	
Sex	100/37	42/42	
Education	13	13.9	
MMSE	28.1 (24-30)	28.2(24-30)	28.1 (24-30)
Processing speed	55.4	50.6	50.3

2. Imaging acquisition and processing

Diffusion weighted imaging (DWI) data were collected on a 3T Discovery MR750 (General Electric) scanner with a 32-channel head coil. Data were acquired using a single-shot, spin-echo-planar, T2-weighted sequence, with a spatial resolution of 0.98 × 0.98 × 2 mm. The sequence parameters were: TR = 8.0 s, 64 slices with no gap in between, 256 × 256 matrix (FOV = 250 mm), 90º flip angle, b = 1000 s/mm2 and six b = 0 images. At baseline and the first follow up, 3 DWI sessions were included for each participant. At the second follow up, only one session was included in the protocol. To retain

consistency in data analyses across multiple time point (T5-T7), only the first scanning session (for baseline and first follow up) were included in the analysis. TE is 84.4 ms at T5 and varied between 81.2 ms to 82.8ms at T6/T7. All participants were examined on the same scanner with no software or hardware update during the data-collection period.

The raw DWI data was first pre-processed using MRtrix 3.0, including denoising, unringing and motion correction, topup, eddy current correction, and bias field correction. We used Synb0 (Schilling et al., 2020) to correct for the spatial distortions caused by susceptibility induced off-resonance fields. This approach synthesizes an undistorted b0 image based on a distorted b0 and a T1 image using deep learning. The ventricles, scalp and nonparenchymal regions within the images were removed using the BET tool as implemented in FSL (Smith, 2002).

We used the constrained spherical deconvolution (CSD; Tournier et al., 2004, 2007) to obtain the Fibre Orientation Distributions (FODs) in each voxel. This was done by first estimating the response functions for single-fiber WM as well as gray matter (GM) and CSF using an unsupervised method (Dhollander et al., 2019). Single-Shell 3-Tissue CSD (SS3T-CSD) was performed to obtain WM-like FODs as well as GM-like and CSF-like compartments in all voxels (Dhollander and Connelly, 2016), using MRtrix3Tissue (https://3Tissue.github.io), a fork of MRtrix3 (Tournier et al., 2019). WM FOD images were then corrected for intensity inhomogeneities and used in the subsequent analyses.

Whole-brain Anatomically Constrained Tractography (ACT, Smith et al., 2012) was performed on the WM FOD images. ACT is an additional module to the streamlines tractography, which uses T1 images as anatomical priors to constrain the streamlines beginning, traversing, and ending in anatomically plausible regions. This was achieved by processing and segmenting the T1-image into 5 different tissue types, cortical GM, sub-cortical GM, WM, CSF, and pathological tissue. The segmented images were aligned to the B0 images for each individual using ANTs and were then feeded into the whole-brain tractography as a mask. ACT improved the biological accuracy of tractography, and greatly decrease false positive streamlines. Ten million tractography streamlines were reconstructed , with the GM–WM interface used as seed regions. The generated tractograms were filtered using Spherical-deconvolution informed filtering of tracks (SIFT2, Smith et al., 2015).

3. Connectome construction

Structural connectomes were generated based on tractograms and the atlas-based parcellation images. The network includes 179 atlas regions/nodes on each cortical hemisphere, based on HCPMMP 1.0, with an additional 16 subcortical regions based on the FreeSurfer segmentation. Two regions in the temporal cortex spans only 2 voxels with no associated streamlines and were therefore excluded in

the analysis. The cerebellum and the brainstem were not included in some images because of restricted field of view and these regions were therefore omitted from further analyses. A novel measurement, fiber bundle capacity (FBC, Smith et al., 2020), was used as to estimate the structural connectivity strength/edges of the network. FBC represents the capacity of a fiber bundle to transfer information. Compared to the commonly used connectivity measures, such as number of streamlines, FBC is reflective of the underlying biological connectivity, i.e., fiber density (Smith et al., 2020), and is less influenced by brain volume or streamline length. Moreover, although the number of streamlines generated in tractography is fixed for each participant, and the volumes of each parcellated brain region is adjusted during the post-analysis, the number of streamlines assigned to a particular pair of parcels might still be biased due to many factors that cannot be controlled for (Smith et al., 2020). Thus, we consider FBC to be a more robust and less biased measure.

Since the distribution of FBC is heavily right-skewed (Figure S1), we used the log-transformed FBC to quantify the connection weights of the network (i.e., network edges) in the analysis. To further minimize false-positive connections, we used two criteria to select connections to be included in subsequent analyses (Arnatkeviciute et al., 2021) (i) connections that are present in at least 30 % of participants; and (ii) amongst the τ % strongest edges to achieve the desired network density. The densities (proportion of non-zero connections) of the mean connectome were 64.4 %, 64.7 %, 68.5 %, 67.4 %, and 57.8 % for age groups. After thresholding (i), the densities of the mean connectome were 46.4 % for all age groups younger than 80 years, and 46.2% for 80-85 group. The density distributions for each participant are shown in Figure S2. Weak connections might introduce randomness that could influence graph-theoretical measurements (van den Heuvel et al., 2017). We therefore examined our main results across a range of densities (τ = 5 %, 10 %, 15 %, 20 %, 25 %, 30%), and on the mean connectome based on these six densities. This ensured that a proportion of weak/false-positive connections were further removed for all the participants after thresholding (ii). Moreover, after thresholding (ii), the density distributions among age groups were different for τ = 15%, 20 %, 25 %, 30% (p-values < 0.05), and were comparable for τ = 5 %, 10 %. Thus, the selection of these thresholds also aims to test whether our findings are affected by the age effects on network densities. The analysis using τ = 30 % were presented in the main results. The replication using τ = 5 %, 10 %, 15 %, 20 %, 25 %, and the mean connectome are reported as supplementary results.

4. Characteristics of the human connectome

To characterize the topographical organization of the connectome, we calculated 3 metrics, degree, rich-club coefficient, and connection distance on the averaged connectome of the baseline sample. Degree was computed for each node as the total number of edges in the network connected to this

node. At a particular degree threshold k, hubs are defined as the nodes with degree > k, and nonhubs are the nodes with degree <= k. Connections are subsequently labeled as rich (hub-hub), feeder (hub-nonhub), and peripheral (nonhub-nonhub) connections. Rich-club coefficient measures the extent to which hub regions in a network connect between each other.

$$\varphi(k) = \frac{2E_{>k}}{N_{>k}(N_{>k} - 1)}$$

where N_k is the number the nodes with degree > k, and E_k are the number of edges among nodes with degree > k (Colizza et al., 2006). Since φ(k) is expected to be larger within nodes with higher degree, φ(k) can be normalized by dividing φ(k) of the random networks. We generated 1000 random null networks while retaining the same network degree, φ_{random}(k) was then computed for each network and averaged.

$$\Phi_{norm}(k) = \frac{\varphi(k)}{\varphi_{random}(k)}$$

Φ_{norm}> 1 indicates a rich-club organization. Statistical significance of Φ_{norm} was tested based on the distribution of the φ_{random}(k). Degree and rich-club coefficients were calculated using the Brain Connectivity Toolbox. Euclidean distance is defined as the straight-line distance between the centroids of pair of regions. This is a commonly used measure of wiring cost of connections.

In addition to defining hubs using degree centrality, an unweighted measurement of connectivity strength, hubs are defined using "hubness", which is based on a sum of several graph metrics, including weighted connectivity strength, path length, weighted betweenness centrality, and weighted clustering-coefficient (Van Den Heuvel et al., 2010). We explored the distribution of "hubness" across regions of the structural brain networks, and also addressed the question if "hubness" resulted in identification of the same regions as those being hubs. To calculate the hubness of each node, we sum the rank of connectivity strength and betweenness centrality in an ascending order, and path length and clustering-coefficient in a descending order. The path length of a node refers to the averaged minimal distance between this node and all the nodes in the network. The equation is:

$$L_i^{weighted} = \frac{\sum_{j \in N, i \neq j} d^{weighted}(i,j)}{N_{>k}(N_{>k} - 1)}$$

with

$$d^{weighted}(i,j) = \sum_{u,v \in g^{w}_{i \Leftrightarrow j}} \frac{1}{w_{uv}}$$

where $g^{w}_{i \Leftrightarrow j}$ is the shortest path between node *i* and *j, and* w_{uv} is the connection weights (i.e., log-transformed FBC) of all pairs of nodes *u* and *v* on the shorted distance $g^{w}_{i \Leftrightarrow j}$. The global efficiency is the average inverse shortest path length in the network. Betweenness centrality of a node is defined as the proportion of the shortest path that passed through this node. The equation is:

$$B_i^{weighted} = \frac{1}{(n-1)(n-2)} \sum_{h,j \in N, h \neq i, j, i \neq j} \frac{sp_{hj}(i)}{sp_{hj}}$$

where $sp_{hj}(i)$ is the number of shortest path in the network that passes through node *i*.
Clustering-coefficient of a node represents the probability that the neighbors of this node are also interconnected.

$$C_i^{weighted} = \frac{\sum_{j,h \in N} (w_{ij} w_{ih} w_{jh})^{1/3}}{k_i(k_i - 1)}$$

where k_i is number of nodes that are connected to node i, and $\frac{1}{2}\sum_{j,h \in N} (w_{ij} w_{ih} w_{jh})^{1/3}$ is the geometric mean of triangles around *i*.

We further investigated whether connectome hubs had higher metabolic rate compared to non-hubs using the brain regional metabolism data provided by a positron emission tomography study (Vaishnavi et al., 2010). In this particular study, several cerebral metabolic measurements, including glycolytic index (GI), cerebral metabolic rate for oxygen (CMRO2), glucose (CMRGlu) and the cerebral blood flow (CBF), were acquired in 33 normal adults during rest. The values of the measurements were then assigned to 82 Brodmann regions in the brain. We related mean connectome degrees to the metabolic measures across regions using Pearson's correlation. Subcortical regions and left and right Brodmann area 26 were excluded from the analysis. Permutation was used to test statistical significance of the correlation against null models. We generated 1000 randomly shuffled brain maps (surrogate maps) with preserved similar spatial autocorrelation (SA) using BrainSMASH (Burt et al., 2020). Pearson correlations were performed between brain map representing the degree and 10.000 randomly shuffled but spatially constrained brain maps. P-values ($P_{permutation}$) smaller than 0.05 were considered as being significant.

5. The influence of age on connectome

5.1 Threshold-free network-based analysis

For cross-sectional analysis, we examined the effect of age on whole brain log-transformed FBC at the edge level (Equation1: $log(FBC) \sim Age + Sex$) using non-parametric permutation testing with the threshold-free network-based statistics (TFNBS, Vinokur et al., 2015) algorithm. This algorithm uses the concept of Threshold Free Cluster Enhancement (TFCE, Smith and Nichols, 2009) to the network domain, and outputs an enhanced matrix based on local cluster extent and magnitude. The enhanced matrix can then be turned into edge-wise p-values using permutation testing. TFNBS is more sensitive than Network Based Statistic (Zalesky et al., 2010), and does not require a hard cluster-forming thresholding. Permutation was performed with n = 5000 data shuffling for statistics inference. We then added an age square term in equation to investigate the quadratic age effects (Equation2: $log(FBC) \sim Age + Age^2 + Sex$). TFNBS was performed in MRtrix3.0. For the longitudinal analysis, we examined changes in structural connectivity from T6 to T7 and the linear age effects on the changes in older adults across 5 years (Equation3: $log(\triangle FBC) \sim Age + Sex$). P-values ($P_{TFNBS}$) smaller than 0.05 were considered as being significant.

5.2 Graph theoretical analyses

We compared the degrees of the connectomes among five age groups (25-45, 50-55, 60-65, 70-75 and 80-85 years), and across time points from T6 to T7. Moreover, we tested the age effect on the overall nodal distribution of degree. This was done by first choosing a degree distribution of the averaged connectome of the 25-45 age bin as a youth-like degree organization, and then calculating the similarity between degree distribution for each participant and the youth-like degree organization using Pearson's correlation. Linear and quadratic age effects on the similarity (correlation coefficients) were estimated using a linear model for all participants from 50 years old. To characterize whether the effect of age on connectivity strength is preferentially stronger in certain types of connections in the human brain, we used linear regression (Equations 1 and 2) to estimate the beta-values of linear and quadratic age effects on mean connectivity of rich, peripheral, and feeder connections across different hub-defined thresholds. Sex was included as a covariate in the analyses. For each type of connection under a specific threshold k, mean connectivity is represented as the sum of log-transformed FBC divided by the number of non-zero connections. Thus, the analysis will not be confounded by the fact that the number of connections was larger for higher degree nodes. Another way of examining the data is to examine whether the edge-wise beta-values are more concentrated in certain types of connections. This was done by comparing beta-values at the edge level among rich, peripheral, and feeder connections across hub-defined thresholds using Welch's t test.

We then related the degree of the connectome to the beta-values of age-effects across nodes to further investigate whether the effects of age are larger on the nodes with higher degrees. The output from TFNBS was a 374 × 374 matrix of beta-values of linear (or quadratic) age effects, which were turned into a vector of 374 mean beta-values by row-wise sum of the matrix divided by the number of non-zero connections. The vector of mean beta-values represents to what extent age influences the average connectivity strength from each node to the rest of the brain. This was then correlated with the degrees of each node using Pearson's correlation. Statistical inferences were based on permutation tests with 10000 SA-preserved surrogate maps.

For the longitudinal analysis, we examined whether the changes and the linear age effects on the changes of connectivity strength (Equation 3) were larger in rich compared to peripheral, or feeder connections. Similar to the cross-sectional analysis, this was done by (1) comparing the longitudinal changes or the age effects on the changes among rich, peripheral, and feeder connections across different hub-defined thresholds; (2) relating the degree of the connectome to the beta-values across nodes. Statistical inferences were based on permutation tests with 10.000 SA-preserved surrogate maps.

In addition to degree, we also explored how other topological properties of the connectomes differed among five age groups, and whether they change from T6 to T7. Several commonly used graph metrics were tested, including path length, global efficiency, betweenness centrality, and clustering coefficient.

6. The relation between structural connectivity and processing speed

The associations between whole brain log-transformed FBC and processing speed were examined using TFNBS controlling for age and sex (Equation 3, $Speed \sim Age + Sex + log(FBC)$). To test whether connections that were linked to hubs are critical for processing speed, we compared the median of the degrees for the regions that demonstrated significant connections associated with speed in the TFNBS analysis with median degree of the rest of the brain. In addition, we investigated whether the connections that were potentially related to speed from TFNBS were more concentrated in rich, peripheral, or feeder connections. This was examined by first identifying hubs/non-hubs based on an arbitrary nodal degree threshold (top 20% of the degree distribution). The averaged beta-values of the associations with speed were compared among rich, peripheral and feeder connections. The statistical inferences were made based on SA-preserved permutation (Burt et al., 2020).

We investigated whether structural connectivity mediates the relation between age and processing speed. Averaged connectivity strength was extracted for the connections that were significantly associated with speed. We estimated the total effect of age on speed, the effect of age

and averaged connectivity strength on speed, and the indirect mediating effect of age on speed via connectivity strength. The confidence interval of the mediation effect was produced using a quasi-Bayesian approximation using the "mediation" package in R (Tingley et al., 2014).

7. Replication and validation

To determine whether our findings are robust, we replicated the analyses using multiple alternative approaches and parameters. First, in our main analysis, we explore whether our main results, the heterogeneous age effects on rich/peripheral/ feeder connections, are robust and replicable based on "hubness" (Van Den Heuvel et al., 2010). Second, the size of individual brain regions can influence the results. We therefore repeated the correlation analysis between the brain maps of degree and the age effects while controlling for regional brain volume. In addition, we replicated out main findings across different connectome density thresholding (τ = 5 %, 10 %, 15 %, 20 %, 25% and the mean connectome based on six density thresholds).

Results

1. Characteristics of the group-level structural network

The averaged structural network, which was based on 137 participants from 25-85 years old has a long-tailed degree distribution (Figure 2A), and the tail of the degree distribution ($k > 115$) follows a power-law (bootstrapped-p > 0.05, Clauset et al., 2009). It suggests that this network is a scale-free network with several hub nodes having high degrees. The nodes with 1 SD above the mean degree (around top 9% highest degree) include the following regions: the bilateral retrosplenial cortex, bilateral thalamus, bilateral putamen, bilateral caudate nucleus, bilateral globus pallidus, bilateral ventral diencephalon, bilateral hippocampus, two regions in the anterior cingulate cortex, one region in the left mid-cingulate, and one region in the left posterior cingulate (Figure 2B). φnorms within these hubs are significantly stronger than expected by chance and increase with the hub-defining threshold k increasing (Figure 2C). This suggests that the network connections demonstrate a rich-club organization, and hubs are more densely connected than chance level. The mean connection distance (a measure of wiring cost) increases as a function of increased hub-defining threshold k, and the mean distance among hubs are significantly larger (one-sided Welch's t-test, $p < 0.05$) than the mean distance of peripheral and feeder connections across multiple thresholds (Figure 2D, black dots). In addition, across 79 Brodmann areas, mean degrees were correlated with several measures of regional brain metabolisms, including GI, $CMRO_2$, CMRGlu, and CBF (Figure 2E). The results

indicate greater metabolic rates in higher-degree compared to lower-degree brain areas across cortical regions.

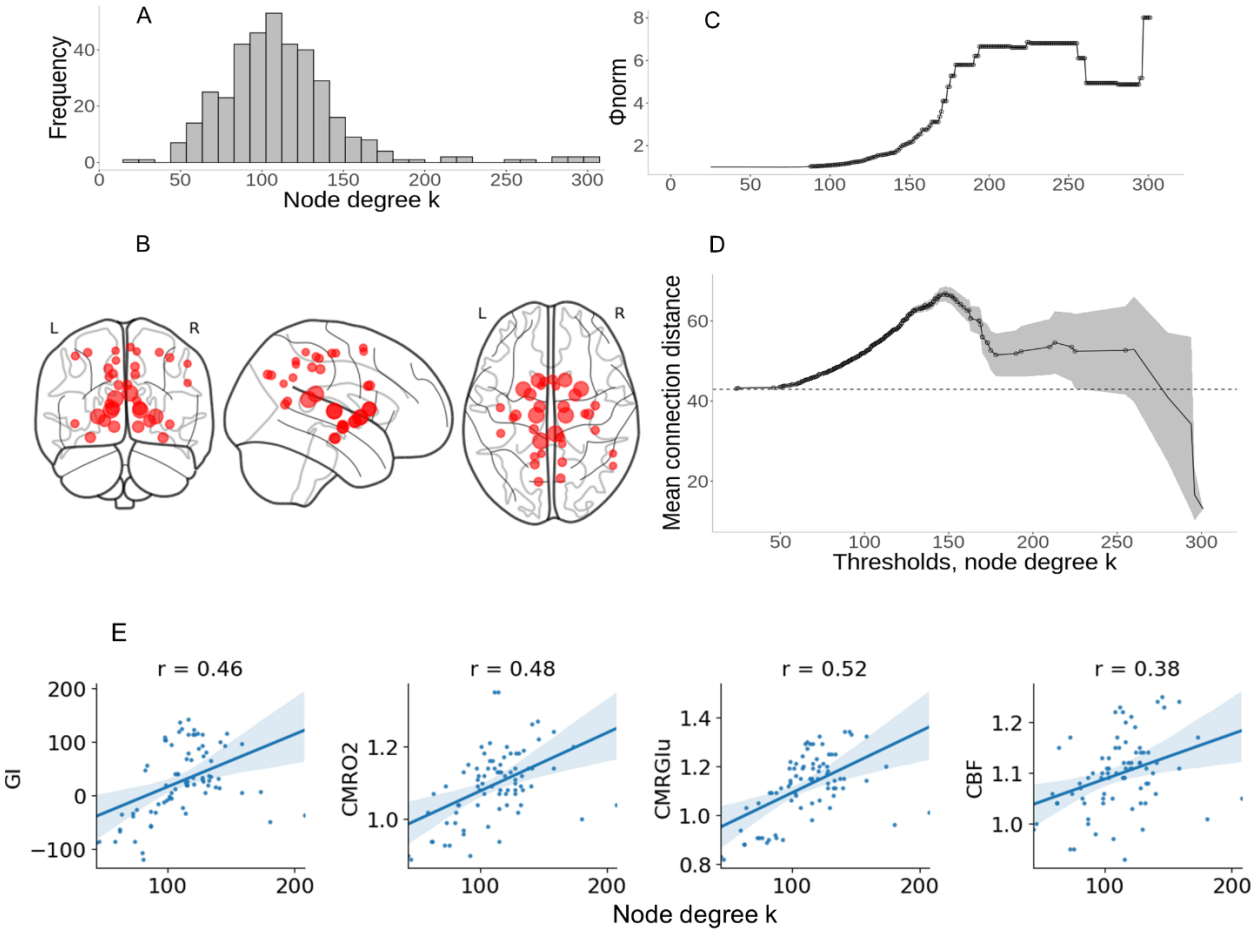

Figure 2. Network characteristics. (A) the long-tailed degree distribution across nodes indicates the presence of a small number of highly connected hubs. (B) The anatomical location of hubs defined by 1SD higher than mean degree; the size indicated the degree of each node. (C) The normalized rich-club coefficient φ norm increases as a function of degree threshold (k) used to define hubs. Black circles indicate significant ($P_{permutation} < 0.05$) φnorm compared to 1000 degree-retained random networks. (D) Mean connection distance among rich club (hub-hub) connections increases as a function of degree threshold (k) used to define hubs. The shaded area depicts two standard errors around the mean. Black circles indicate significant larger distance among rich club connections compared to averaged feeder and peripheral connections. The dashed line shows the average connection distance across all network links. (E) Mean degrees are correlated with glycolytic index (GI, Pearson's $r(77) = 0.46$, $P_{permutation} < 0.05$), the cerebral metabolic rate for oxygen (CMRO2, Pearson's $r(77) = 0.48$, $P_{permutation} < 0.05$), cerebral metabolic rate for glucose (CMRGlu, Pearson's $r(77) = 0.52$, $P_{permutation} < 0.05$), and the cerebral blood flow (CBF, Pearson's $r(77) = 0.38$, $P_{permutation} < 0.05$). The statistical significances of Pearson's correlation coefficients were based on 1000 permutation tests.

Degree was highly correlated with hubness, and with the other three measures of centrality, i.e., path length, betweenness centrality, and clustering-coefficient (Figure S3A). Hubs defined by degree are also consistently ranked for the measure of hubness (Figure S3B). The nodes with top 1 SD above mean hubness are as follows: the bilateral retrosplenium cortex, bilateral hippocampus, bilateral pallidum, bilateral ventral diencephalon, three regions in the bilateral posterior cingulate, bilateral thalamus, bilateral amygdala, and bilateral mid- cingulate. Those regions are fully covered by the hubs defined using nodal degree. However, caudate and putamen were defined as hubs according to their high degree but were not hubs if using "hubness" as a definition, due to their relatively low betweenness centrality.

2. The influence of age on the brain connectome

Degrees are highly correlated and the identified hubs (brain regions with 1 SD higher than the mean degree) were similar across age bins and across the five-year time interval, suggesting relative stable spatial distributions of hubs in healthy adults of different ages. However, there is a significant age effect on the youth-like degree distributions, indicating that older participants have less youth-like degree distribution ($p < 0.001$). The distributions of the degrees between pairs of age bins/time points are presented in Figure S4. Anatomical locations of hubs for five age groups are presented in Figure S5.

2.1 Cross-sectional results

TFNBS analyses showed both significant linear (Figure 3A) and quadratic (Figure 4A) age effects on multiple cortical-cortical connections and most of the cortical-subcortical connections, suggesting that older adults had globally lower structural connectivity strength compared to younger adults. More importantly, results showed that both of the linear (Figure 3B) and quadratic (Figure 4B) age effects were largest for hub connections compared to peripheral, and feeder connections regardless of the thresholds used to define hubs. The linear age effects in hub connections with thresholds k from 24 to 260, and feeder connections with k from 51 to 301 are significantly larger than the peripheral connections. The quadratic age effects in hub connections with thresholds k from 46 to 280, and feeder connections with k from 51 to 301 are significantly larger than the peripheral connections. Mean linear/quadratic beta values were also larger for rich connections compared to feeder (linear: $P < 0.005$ for $175 > k > 46$; quadratic: $P < 0.005$ for $168 > k > 85$) and peripheral connections (linear: $P < 0.0001$ for $k > 102$; $P < 0.005$ for $k > 103$) across hub-defining thresholds (Figure S6). This suggests that higher negative beta-values are mostly concentrated in rich links, compared to feeder or peripheral links. In addition, we found significant correlation between the degrees and the averaged

beta-values of the age effects ($P_{permutation} < 0.0001$, r = -0.496 for linear age effects; $P_{permutation} < 0.05$, r = -0.352 for quadratic age effects), indicating that brain regions with higher degree also have larger age-effects from a particular brain region to the rest of the brain (Figures 5A and 6A).

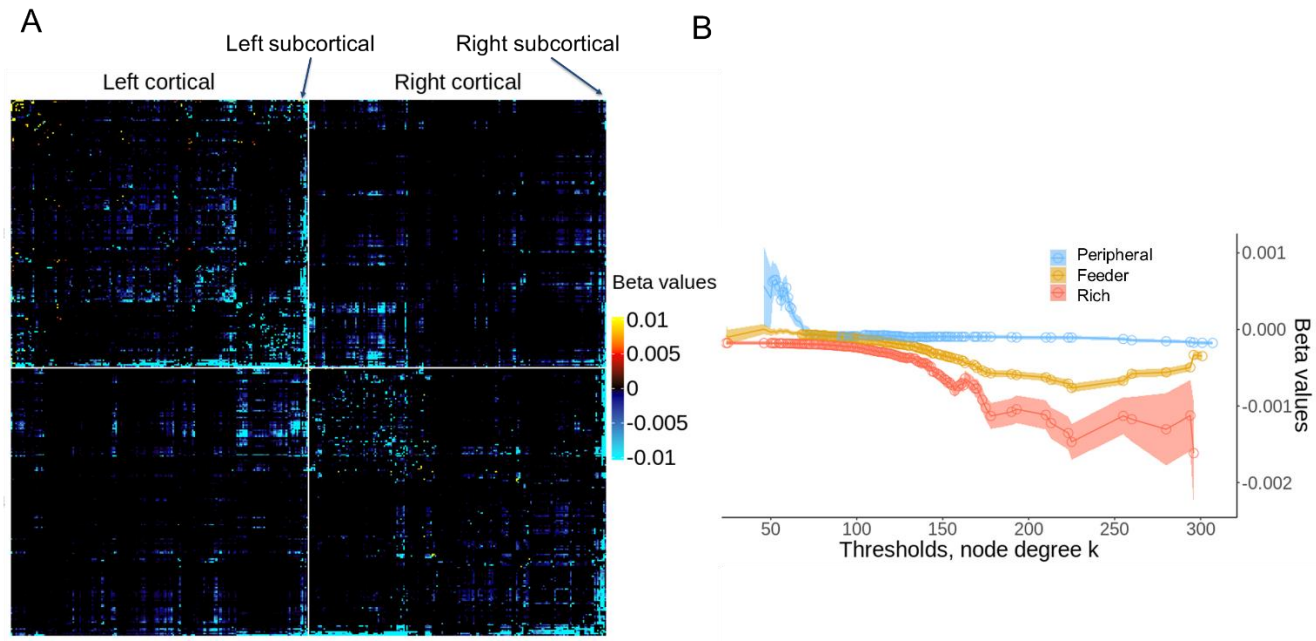

Figure 3. Linear age effects on the whole-brain connectome. (A) Significant ($P_{TFNBS} < 0.05$) age effects on connectivity matrix at the edge level. The parcellations are divided into 2 parts, left and right hemisphere, and are displayed as: left cortical, left subcortical, right cortical, and right subcortical brain regions. (B) The beta values of averaged connectivity for rich (hub–hub), feeder (hub–nonhub), peripheral (nonhub–nonhub) connections as a function of the thresholds, k, used to define hubs. Shaded area is one standard error around the mean. Circles represents significant beta-values at a given threshold.

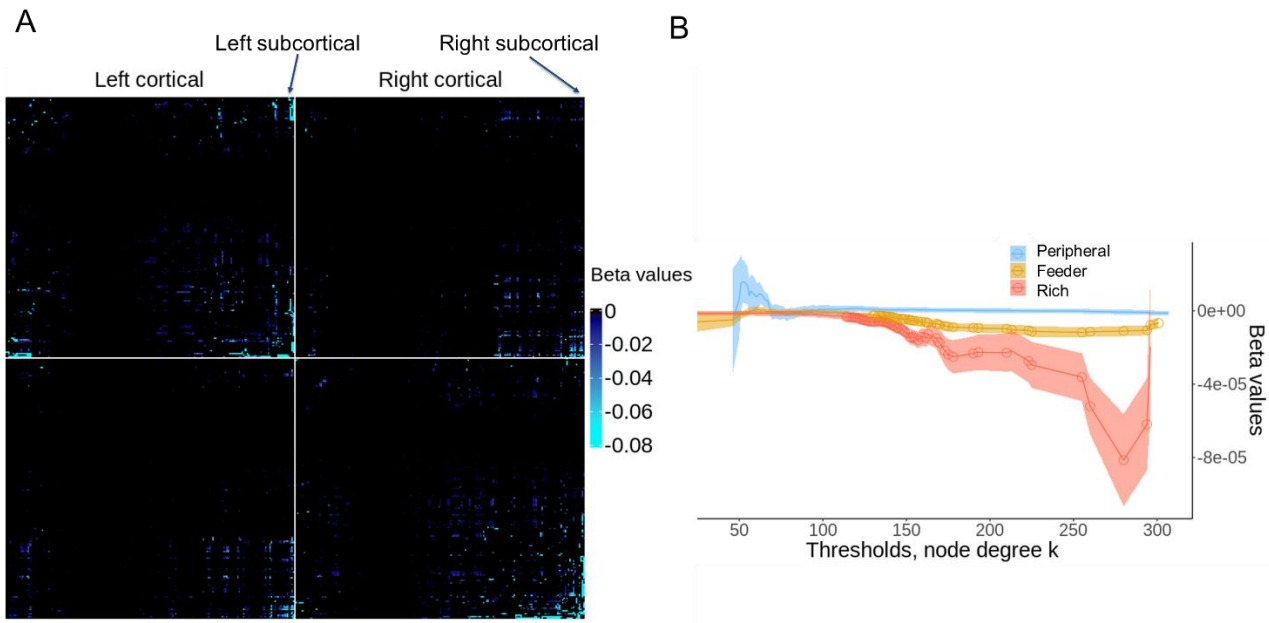

Figure 4. Quadratic age effects on the whole-brain connectome. (A) Significant (P_{TFNBS} <0.05) age effects on connectivity matrix at the edge level. The parcellations are divided into 2 parts, left and right hemisphere, and are ordered as left cortical, left subcortical, right cortical, and right subcortical brain regions. Only negative quadratic age effects are significant, and positive beta-values are therefore not displayed. (B) The beta values of averaged connectivity for rich (hub–hub), feeder (hub–nonhub), peripheral (nonhub–nonhub) connections as a function of the thresholds, k, used to define hubs. Shaded area is one standard error around mean. Circles represents significant beta-values at a given threshold.

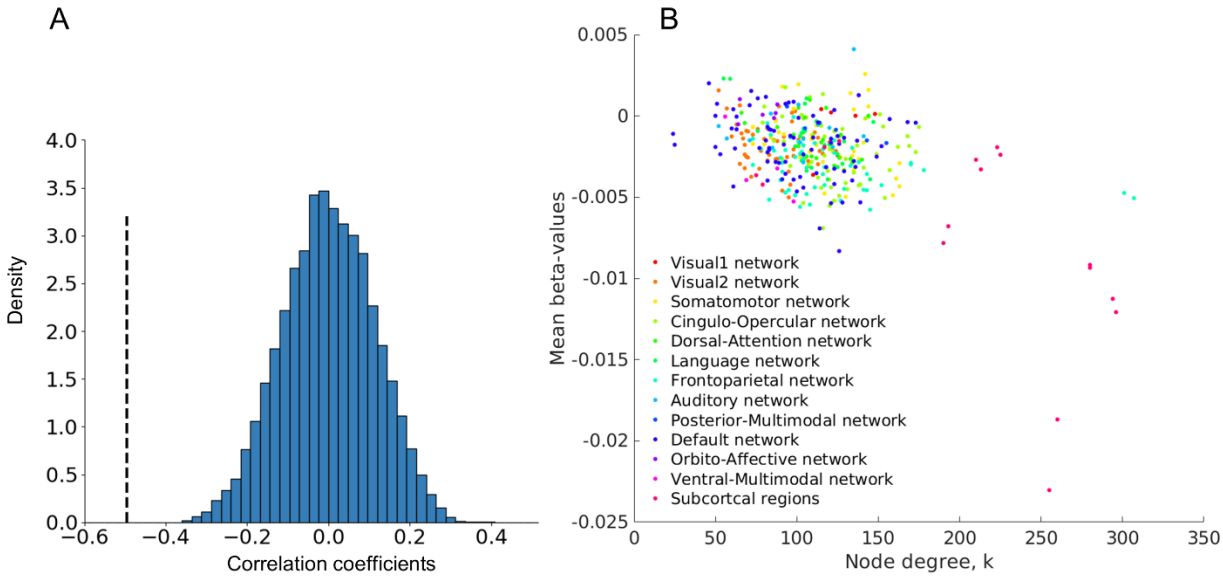

Figure 5. The distribution of Pearson's correlations between degree and surrogate brain maps (A). The surrogate brain maps were generated randomly while preserving the same spatial autocorrelation (SA) as the brain map of the averaged linear age effects. The dashed lines represent the true

correlations based on our data. (B) Scatter plot of nodal degrees and the averaged beta-effects. Colors represent functionally defined networks in cortical regions and sub-cortical brain regions.

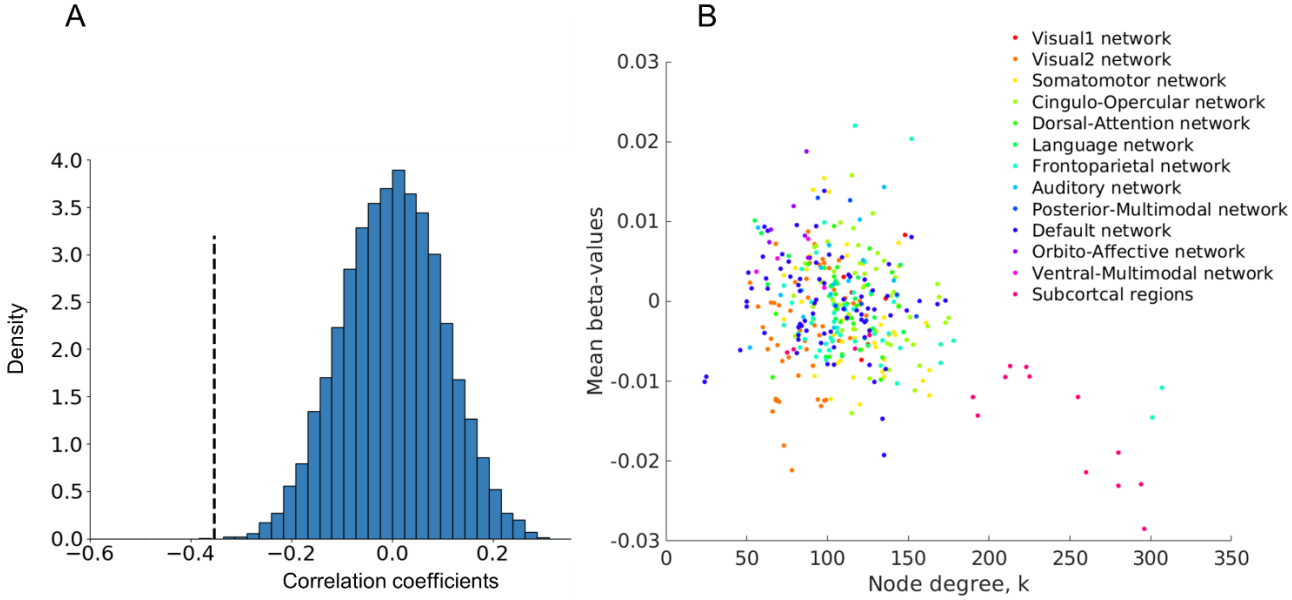

Figure 6. The distribution of Pearson's correlations between degree and surrogate brain maps (A). The surrogate brain maps were generated randomly while preserving the same SA as the brain map of the averaged quadratic age effects. The dashed lines represent the true correlations based on our data. (B) Scatter plot of nodal degrees and the averaged quadratic beta-effects. Colors represent functionally defined networks in cortical regions and sub-cortical brain regions.

Since many sub-cortical regions have both high degree as well as large age effects (Figures 5B and 6B), it is possible that the significant spatial correlation between brain maps of the degree and the age effects is driven by the sub-cortical regions. Thus, we repeated the correlation analysis in only cortical regions. The network characterizations of brain networks for only cortical regions are shown in Figure S7. We were able to replicate the results showing a significant spatial correlation between the degrees and the averaged beta-values ($r = -0.286$, $n = 358$; Figure S8). For the quadratic effects, a similar, albeit somewhat weaker, results pattern was found. The correlations for the quadratic effects were found significant in the language network ($r = -0.54$), frontal-parietal network ($r = -0.3$), posterior-multimodal network ($r = -0.596$), and sub-cortical brain regions ($r = -0.817$). A marginally significant spatial correlation between the degrees and the averaged beta-values ($P_{permutation} < 0.07$, $r = -0.173$) was found for the analysis that was conducted for only cortical regions (Figure S9).

In addition to connectivity strength, we found lower clustering coefficient and global efficiency, and higher path length and betweenness centrality in older compared to younger adults (p-values < 0.00001). Interestingly, the age effects on clustering coefficient, path length and betweenness centrality were larger in hub compared to non-hub brain regions (p-values < 0.0001, Figure S10).

2.2 Longitudinal results

Results show that across five years, there was a significant decline in structural connectivity (log-transformed FBC) in multiple cortical-cortical connections, as well as cortical-subcortical connections. There were larger changes in intra-hemispheric connections compared to the inter-hemispheric connections. The changes were more pronounced for rich connections compared to feeder and peripheral connections (Figure 7). We also found a weak but significant age effect on the changes of structural connectivity, mainly in rich connections (Figure S11). This result replicated the quadratic age effects and indicates that older adults had larger decline compared to younger adults, and that this age-related difference in decline was most pronounced in rich connections. A correlation analysis showed a significant spatial correspondence between brain maps of the degree and the changes of structural connectivity (Figure S12). A similar pattern of results was found for the age effects on the changes (Figure S13). The longitudinal results generally replicated the main findings of the cross-sectional analysis and suggests that the decline of the structural connectivity in older adults are largest and more concentrated in rich connections. However, compared to cross-sectional analysis, the longitudinal results demonstrated greater discrepancy in changes between intra- and inter- hemispheric connections. In addition to connectivity strength, we found declined clustering coefficient and global efficiency, and increased higher path length and betweenness centrality across five years (p-values < 0.00001). The longitudinal changes were greater on betweenness centrality in hub compared to non-hub brain regions (p-value < 0.01, Figure S14).

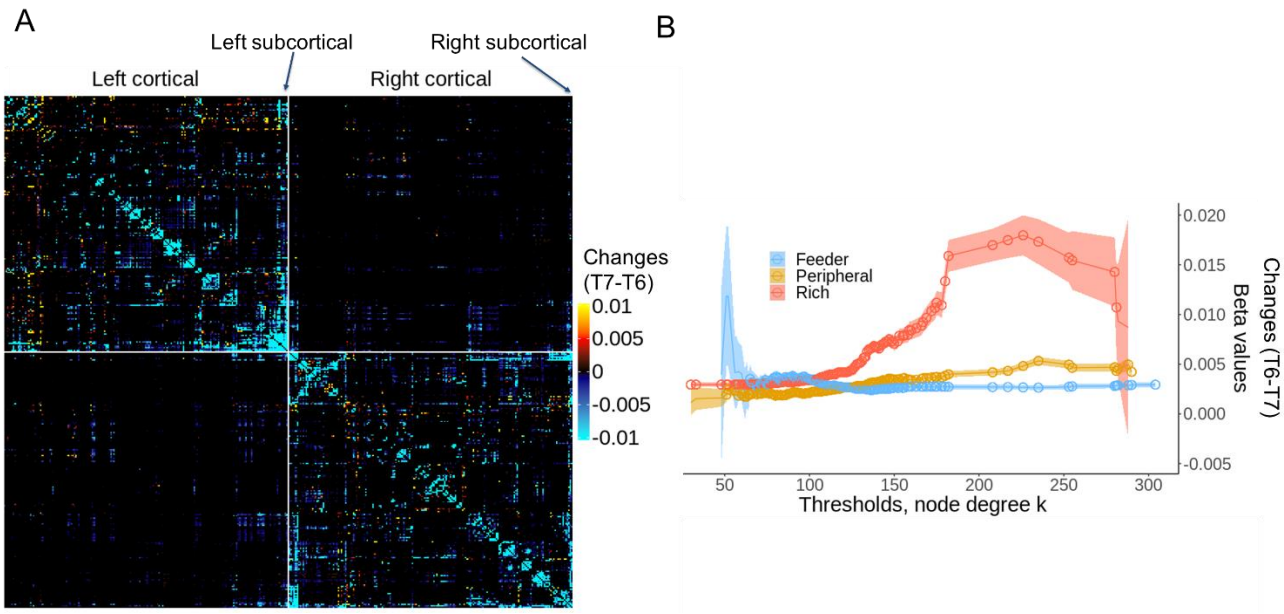

Figure 7. The changes on whole-brain connectome. (A) Significant (P_{TFNBS} < 0.05) changes on connectivity matrix at the edge level. The parcellations are divided into 2 parts, left and right hemisphere, and are ordered as left cortical, left subcortical, right cortical, and right subcortical brain regions. For illustrative purpose, negative changes (T7 – T6) was used in the plot. (B) The averaged

connectivity changes for rich (hub–hub), feeder (hub–nonhub), peripheral (nonhub–nonhub) connections as a function of the thresholds, k, used to define hubs. Shaded area is 1 standard error around mean. Circles represents significant changes at a given threshold.

3. The relation between structural connectivity and processing speed

TFNBS analyses showed significant associations between multiple cortical/sub-cortical structural connections and processing speed. The associations were found in the connections among somatosensory and motor areas, inferior frontal cortex, inferior and superior parietal cortex, lateral temporal cortex, the temporo-parieto-occipital junction, posterior opercular area, auditory areas, and a subcortical region in ventral diencephalon (Figure S15A). A majority (13 out or 14) of the connections that were significantly ($P_{TFNBS} < 0.05$) associated with speed, also had significant ($P_{TFNBS} < 0.05$) linear or quadratic age effects.

We tested if the significant connections were more concentrated in hub-hub connections. The median of degrees for the brain regions of 14 significant connections is 197, which is significantly larger than expected by chance ($P_{permutation} < 0.0001$, Figure S15B), indicating that brain regions with larger degrees were also the ones that were significantly related to processing speed. We also found that the mean beta-value that was associated with processing speed within the rich connections was significantly larger than the null distribution ($P_{permutation} < 0.001$), whereas the mean beta-value within the peripheral connections is significantly lower than the null distribution ($p < 0.001$, Figure S15C). However, it should be noted that this analysis was conducted on the whole network, not only within the 14 connections that showed significant associations with speed. These results suggest that the largest associations between structural connectivity and processing speed are concentrated in rich connections within a brain network. The significant mediation effect ($p < 0.0001$) showed that 16.7% of the total effect between age and processing speed can be explained by age differences in connectivity strength.

Using longitudinal data, we also tested the change-change associations between connectivity and processing speed from baseline to follow-up using TFNBS controlling for age and sex ($\triangle Speed \sim Age + Sex + log(\triangle FBC)$). However, no significant change-change correlation was found between FBC and processing speed across five years.

4. Validation

Instead of degree, the analysis using hubness to define the level of central/influential of brain regions in the network still showed that the age effects were largest in rich connections, compared to feeder

or peripheral connections (Figure S16). We also tested if the associations between brain maps of the degrees and the beta-values of age / speed are significant after controlling for the brain volumes. Indeed, we were able to replicate our finding using different parcellations, connectome thresholds, or the definitions of connectivity strength (Figure S17). These supplementary analyses show that the pattern of results replicate well and are not influenced by differences in hub definition or parameters used during analysis.

Discussion

Here we demonstrate that the human structural brain network has a rich-club organization with a long-tailed degree distribution. This indicates that the brain network is not random, but rather characterized as a scale-free network. Three main findings were obtained in the current study. First, although the spatial distributions of hubs in the structural brain network are relative stable across age, the connectivity strength within hub regions have larger linear/quadratic age effects compared to non-hub regions. These findings were supported by both cross-sectional and longitudinal analyses. Second, the associations between connectivity strength and processing speed were larger in hub compared to non-hub connections. Third, age-related differences in connectivity strength within hub-hub connections accounts for lower processing speed in older adults. These findings provide evidence that hubs in structural brain networks are more affected by normal aging, and that alterations in hub-hub connectivity partly explain age-related deficits in processing speed in older adults.

Using a novel measurement of connectivity, fiber bundle capacity, current characterization of structural network properties, largely replicates previous results from different samples and various connectivity measurements, including diffusion-tensor based FA and number of streamline counts (Alexander-Bloch et al., 2013; Arnatkeviciute et al., 2021; Crossley et al., 2014; van den Heuvel and Sporns, 2011). This suggests high reproducibility of the rich-club organization of the human connectome. The current results extend these previous observations by demonstrating a less youth-like degree distribution with advancing age, and that the clustering coefficient, global efficiency, path length, and betweenness centrality differed between younger and older adults, especially within hub connections. Together, these results indicate an age-invariant spatial distributions of structural hubs in older adults, but also alterations of the whole-brain topological organization in older adults.

We also found that the mean distance of connections increases as a function of increasing degree, and that the degrees are related to multiple measures of regional brain metabolism. These results are consistent with previous studies (Arnatkeviciute et al., 2021; Crossley et al., 2014; Xu et al., 2022), indicating that hub connections are mainly long-range connections, and have anatomically higher energy cost compared to peripheral regions in the brain.

The cross-sectional TFNBS analysis demonstrated widespread age effects on structural connectivity strength, as indicated by lower FBC with increasing age. Similar results were observed in the longitudinal analysis, showing that FBC declined globally across five years in older adults. These results corroborate previous findings of age effects in multiple indicators of WM microstructure, including WM integrity (e.g., Sexton et al., 2014), WM fiber density (Choy et al., 2020), and number of streamline counts (Coelho et al., 2021). Together with the present results, these findings indicate robust and replicable effects of age on WM microstructure across measurements and using different biophysical models of water diffusion. The finding of lower structural connectivity strength in older compared to younger adults also support previous computational work showing that the degree to which structural brain networks rely on geometric wiring rules is weakened with advancing age (Betzel et al., 2016; Zuo et al., 2017). This finding may also indicate less structural constraints on functional brain organization with advancing age, which might lead to disassociation of the topographical organizations between structural and function connectivity in older adults (Coelho et al., 2021; Zamani Esfahlani et al., 2022).

Importantly, the current results extend previous observations by demonstrating that the age effects on structural connectivity are heterogeneous, with more pronounced effects in rich connections compared to peripheral connections. This pattern was consistent (i) across thresholds and (ii) irrespectively of methods used for defining hubs. Previous computational work has shown that the complex scale-free network has extremely high tolerance for errors (Albert et al., 2000). Thus, complex networks, including brain networks, are highly robust and stable against random attacks. However, this type of network is also sensitive to damage in hubs (Albert et al., 2000). Our results suggested that hubs and rich connections are deferentially more susceptible to the aging process compared to peripheral nodes/connections. Since hub-hub connections are generally long-range connections, they are especially important for efficient global brain communication (Van Den Heuvel et al., 2012). Weakened connections in hub regions might therefore lead to decreased integration and increased segregation of the brain networks, which support previous findings by Coelho et al. (2020). Moreover, when the modeled pathological attack targeted high-degree nodes in the brain network, global efficiency deteriorated more rapidly compared to when nodes were targeted randomly (Crossley et al., 2014). Thus, age-related effects on hub connectivity might explain lower global network efficiency in older compared to younger adults.

While structural connectivity patterns from cross-sectional and longitudinal analyses largely converged, some differences were also identified. Longitudinal results showed larger effects of time on intra- hemispheric compared to inter- hemispheric connections. One possible reason for this difference is that, compared to cross-sectional data, longitudinal analyses might be less influenced by confounding factors, such as cohort effects (e.g., education and nutrition). Additional longitudinal

studies are clearly needed to characterize age-related changes in intra- and inter-hemispheric network connectivity.

It is currently not clear why the effect of age is selectively larger in hub regions of the connectome compared to peripheral connections. There might be several potential explanations. First, since hub connections are generally longer and have been associated with higher blood flow and/or metabolic rate, they might be biologically more expensive to maintain in terms of organization and normal functioning. It is therefore possible that during the normal aging processing, oxidative stress and energy depletion induced by the accumulation of RONCS have a particular impact on hubs because of their higher demands for energy and vulnerability to oxidative stress. Second, since older adults have lower endogenous dopamine (DA) level and DA D1/D2 receptor density compared to younger adults (for a review, see Karrer et al., 2017), a lower level of dopamine could result in altered WM connectivity. In support of this view, some studies have linked DA function with WM integrity. For example, it has been shown that individuals who carried *COMT*-Val allele, which has been associated with lower DA level in the prefrontal cortex, also have lower WM integrity (Li et al., 2022). Animal work has also shown that DA-depleted rats have decreased length of dendrites, as well as altered neuronal density (Kalsbeek et al., 1989, 1987; Wang and Deutch, 2008). Moreover, there have been well-established links between dopamine D1 (Johansson et al., 2022), D2 (Karalija et al., 2019), and DA transporter (Rieckmann et al., 2016) to WM lesion. In the current study, we note that brain regions associated with the high dopamine D1/D2 receptor availability, such as the basal ganglia and the prefrontal cortex also have higher degrees compared to other brain regions. It is therefore possible that age-related decline of DA in these regions contribute to deterioration of the WM fibers, which may partly lead to more deleterious age effect on connections of high-degree nodes.

Hubs are not only located centrally from a topological perspective but are also critical for human cognition. Consistent with previous studies, we found that structural connectivity was associated with processing speed (Zimmermann et al., 2018). The current results add new information about the link between cognitive performance and WM integrity by demonstrating that the connections that were associated with speed performance were linked to brain regions with higher degree than expected by chance. This suggests that regions with higher degrees might be particularly important for integrating information across the brain through long-distance connections in order to increase global network efficiency. Higher brain global efficiency has been related to better cognitive performance in functional resting-state MRI studies (Gießing et al., 2013; Van Den Heuvel et al., 2009). Thus, our results suggest that high-degree regions are important for processing speed, and that age-related differences in connectivity strength in those regions may partly explain deficits in processing speed in older adults. Processing speed is a basic cognitive function, which has been highly correlated with other higher-order cognition, such as working memory and fluid intelligence

(Ackerman et al., 2002; Salami et al., 2018; Waters and Caplan, 2005). This conclusion was confirmed by our finding of significant global correlation between degree distribution and associations connectivity strength with speed, further supporting that high-degree regions are critical for higher-order cognition

While we believe that the current study has several strengths, including a relatively large sample size with a wide age-range, and the availability of both cross-sectional and longitudinal data, a few limitations should be highlighted. First, in this study we focused on degrees and hubs, which are the key characters in graph theory, as indicators of structural connectivity. However, there are many other important topological properties, such as small-worldness and modularity, which reflect different aspects of human connectome organization. Future studies are clearly needed to explore how these properties relate to each other, how they are affected by adult aging and their association with various cognitive functions. We believe that a more systematic characterization based on multiple measures of connectome organization could provide a deeper understanding about the complex human network, and how age might influence those properties of the network. Second, the organization and characteristics of the structural and functional brain networks are similar but not entirely identical. Here we specifically examined intrinsic structural brain network organization, and we therefore lack information on how these results translate to the functional dynamics of hub organization. Future studies that include multimodal assessment of the human connectome are required to explore the age effects on structure-function relationships and how such structure-function associations related to cognitive functioning.

Conclusion

The existing studies showed that brain structural network is a complex, scale-free network with rich-club organization. Using a novel measurement of structural connectivity strength, fiber bundle capacity, the current study replicated previous findings of the topographical characteristics of the human connectome as a complex, scale-free network with rich-club organization in a large sample size with wide age range. By combining network-based and graph-theoretical analyses, we extend previous findings by showing age-related alterations in structural connectivity strength, along with relative unchanged spatial brain network distributions of hubs with advancing age. Importantly, results from both cross-sectional and longitudinal analyses demonstrate that the connections between hubs are more strongly influenced by aging compared to peripheral regions, which might explain the alterations of whole-brain topological organizations in older adults. In addition, we found that the age-differences in hub connections are behaviorally meaningful and mediates the effect of age on processing speed.

References

Achard, S., Bullmore, E., 2007. Efficiency and Cost of Economical Brain Functional Networks. PLOS Comput. Biol. 3, e17.

Ackerman, P.L., Beier, M.E., Boyle, M.O., 2002. Individual differences in working memory within a nomological network of cognitive and perceptual speed abilities. J. Exp. Psychol. Gen. 131, 567–589. https://doi.org/10.1037/0096-3445.131.4.567

Albert, R., Jeong, H., Barabás, A.-L., 2000. Error and attack tolerance of complex networks. Nature 406, 378–382.

Alexander-Bloch, A., Giedd, J.N., Bullmore, E., 2013. Imaging structural co-variance between human brain regions. Nat. Rev. Neurosci. 14, 322–336. https://doi.org/10.1038/nrn3465

Andersson, P., Li, X., Persson, J., 2022. The association between control of interference and white-matter integrity: A cross-sectional and longitudinal investigation. Neurobiol. Aging 114, 49–60. https://doi.org/10.1016/j.neurobiolaging.2022.03.002

Arnatkeviciute, A., Fulcher, B.D., Oldham, S., Tiego, J., Paquola, C., Gerring, Z., Aquino, K., Hawi, Z., Johnson, B., Ball, G., Klein, M., Deco, G., Franke, B., Bellgrove, M.A., Fornito, A., 2021. Genetic influences on hub connectivity of the human connectome. Nat. Commun. 12, 1–14. https://doi.org/10.1038/s41467-021-24306-2

Betzel, R.F., Avena-Koenigsberger, A., Goñi, J., He, Y., de Reus, M.A., Griffa, A., Vértes, P.E., Mišic, B., Thiran, J.P., Hagmann, P., van den Heuvel, M., Zuo, X.N., Bullmore, E.T., Sporns, O., 2016. Generative models of the human connectome. Neuroimage 124, 1054–1064. https://doi.org/10.1016/j.neuroimage.2015.09.041

Buckner, R.L., Krienen, F.M., 2013. The evolution of distributed association networks in the human brain. Trends Cogn. Sci. 17, 648–665. https://doi.org/10.1016/j.tics.2013.09.017

Buckner, R.L., Sepulcre, J., Talukdar, T., Krienen, F.M., Liu, H., Hedden, T., Andrews-Hanna, J.R., Sperling, R.A., Johnson, K.A., 2009. Cortical hubs revealed by intrinsic functional connectivity: Mapping, assessment of stability, and relation to Alzheimer's disease. J. Neurosci. 29, 1860–1873. https://doi.org/10.1523/jneurosci.5062-08.2009

Burt, J.B., Helmer, M., Shinn, M., Anticevic, A., Murray, J.D., 2020. Generative modeling of brain maps with spatial autocorrelation. Neuroimage 220. https://doi.org/10.1016/j.neuroimage.2020.117038

Chan, M.Y., Park, D.C., Savalia, N.K., Petersen, S.E., Wig, G.S., 2014. Decreased segregation of brain systems across the healthy adult lifespan. Proc. Natl. Acad. Sci. U. S. A. 111, E4997–E5006. https://doi.org/10.1073/pnas.1415122111

Chen, Z.J., He, Y., Rosa-Neto, P., Gong, G., Evans, A.C., 2011. Age-related alterations in the modular organization of structural cortical network by using cortical thickness from MRI.

Neuroimage 56, 235–245. https://doi.org/10.1016/j.neuroimage.2011.01.010

Choy, S.W., Bagarinao, E., Watanabe, H., Ho, E.T.W., Maesawa, S., Mori, D., Hara, K., Kawabata, K., Yoneyama, N., Ohdake, R., Imai, K., Masuda, M., Yokoi, T., Ogura, A., Taoka, T., Koyama, S., Tanabe, H.C., Katsuno, M., Wakabayashi, T., Kuzuya, M., Hoshiyama, M., Isoda, H., Naganawa, S., Ozaki, N., Sobue, G., 2020. Changes in white matter fiber density and morphology across the adult lifespan: A cross-sectional fixel-based analysis. Hum. Brain Mapp. 41, 3198–3211. https://doi.org/10.1002/hbm.25008

Clauset, A., Shalizi, C.R., Newman, M.E.J., 2009. Power-law distributions in empirical data. SIAM Rev. 51, 661–703. https://doi.org/10.1137/070710111

Coelho, A., Fernandes, H.M., Magalhães, R., Moreira, P.S., Marques, P., Soares, J.M., Amorim, L., Portugal-Nunes, C., Castanho, T., Santos, N.C., Sousa, N., 2021. Reorganization of brain structural networks in aging: A longitudinal study. J. Neurosci. Res. 99, 1354–1376. https://doi.org/10.1002/jnr.24795

Colizza, V., Flammini, A., Serrano, M.A., Vespignani, A., 2006. Detecting rich-club ordering in complex networks. Nat. Phys. 2, 110–115. https://doi.org/10.1038/nphys209

Crossley, N.A., Mechelli, A., Scott, J., Carletti, F., Fox, P.T., Mcguire, P., Bullmore, E.T., 2014. The hubs of the human connectome are generally implicated in the anatomy of brain disorders. Brain 137, 2382–2395. https://doi.org/10.1093/brain/awu132

Dhollander, T., Connelly, A., 2016. A novel iterative approach to reap the benefits of multi-tissue CSD from just single-shell (+b=0) diffusion MRI data Review of Fixel-Based Analysis (FBA) of diffusion MRI (dMRI) View project Brain network disruption in chronic stroke patients View project.

Dhollander, T., Mito, R., Raffelt, D., Connelly, A., 2019. Improved white matter response function estimation for 3-tissue constrained spherical deconvolution.

Eguíluz, V.M., Chialvo, D.R., Cecchi, G.A., Baliki, M., Apkarian, A.V., 2005. Scale-free brain functional networks. Phys. Rev. Lett. 94, 1–4. https://doi.org/10.1103/PhysRevLett.94.018102

Finkel, D., Reynolds, C.A., McArdle, J.J., Pedersen, N.L., 2005. The longitudinal relationship between processing speed and cognitive ability: Genetic and environmental influences. Behav. Genet. 35, 535–549. https://doi.org/10.1007/s10519-005-3281-5

Gießing, C., Thiel, C.M., Alexander-Bloch, A.F., Patel, A.X., Bullmore, E.T., 2013. Human brain functional network changes associated with enhanced and impaired attentional task performance. J. Neurosci. 33, 5903–5914. https://doi.org/10.1523/jneurosci.4854-12.2013

Gong, G., Rosa-Neto, P., Carbonell, F., Chen, Z.J., He, Y., Evans, A.C., 2009. Age- and gender-related differences in the cortical anatomical network. J. Neurosci. 29, 15684–15693. https://doi.org/10.1523/jneurosci.2308-09.2009

Hill, J., Inder, T., Neil, J., Dierker, D., Harwell, J., Van Essen, D., 2010. Similar patterns of cortical expansion during human development and evolution. Proc. Natl. Acad. Sci. U. S. A. 107, 13135–13140. https://doi.org/10.1073/pnas.1001229107

Johansson, J., Nordin, K., Pedersen, R., Karalija, N., Papenberg, G., Andersson, M., Korkki, S.M., Riklund, K., Guitart-Masip, M., Rieckmann, A., Bäckman, L., Nyberg, L., Salami, A., 2022. Bi-phasic patterns of age-related differences in dopamine D1 receptors across the adult lifespan. bioRxiv 1–35.

Kalsbeek, A., Buijs, R.M., Hofman, M.A., Matthijssen, M.A.H., Pool, C.W., Uylings, H.B.M., 1987. Effects of neonatal thermal lesioning of the mesocortical dopaminergic projection on the development of the rat prefrontal cortex. Dev. Brain Res. 32, 123–132. https://doi.org/10.1016/0165-3806(87)90145-3

Kalsbeek, A., Matthijssen, M.A.H., Uylings, H.B.M., 1989. Morphometric analysis of prefrontal cortical development following neonatal lesioning of the dopaminergic mesocortical projection. Exp. Brain Res. 78, 279–289. https://doi.org/10.1007/BF00228899

Karalija, N., Wåhlin, A., Ek, J., Rieckmann, A., Papenberg, G., Salami, A., Brandmaier, A.M., Köhncke, Y., Johansson, J., Andersson, M., Axelsson, J., Orädd, G., Riklund, K., Lövdén, M., Lindenberger, U., Bäckman, L., Nyberg, L., 2019. Cardiovascular factors are related to dopamine integrity and cognition in aging. Ann. Clin. Transl. Neurol. 6, 2291–2303. https://doi.org/10.1002/acn3.50927

Karrer, T.M., Josef, A.K., Mata, R., Morris, E.D., Samanez-Larkin, G.R., 2017. Reduced dopamine receptors and transporters but not synthesis capacity in normal aging adults: a meta-analysis. Neurobiol. Aging 57, 36–46. https://doi.org/10.1016/j.neurobiolaging.2017.05.006

Li, X., Salami, A., Avelar-Pereira, B., Bäckman, L., Persson, J., 2022. White-Matter Integrity and Working Memory: Links to Aging and Dopamine-Related Genes. eNeuro 9. https://doi.org/10.1523/ENEURO.0413-21.2022

Liang, X., Zou, Q., He, Y., Yang, Y., 2013. Coupling of functional connectivity and regional cerebral blood flow reveals a physiological basis for network hubs of the human brain. Proc. Natl. Acad. Sci. U. S. A. 110, 1929–1934. https://doi.org/10.1073/pnas.1214900110

Nilsson, L.G., Bäckman, L., Erngrund, K., Nyberg, L., Adolfsson, R., Bucht, G., Karlsson, S., Widing, M., Winblad, B., 1997. The betula prospective cohort study: Memory, health, and aging. Aging, Neuropsychol. Cogn. 4, 1–32. https://doi.org/10.1080/13825589708256633

Nyberg, L., Boraxbekk, C.J., Sörman, D.E., Hansson, P., Herlitz, A., Kauppi, K., Ljungberg, J.K., Lövheim, H., Lundquist, A., Adolfsson, A.N., Oudin, A., Pudas, S., Rönnlund, M., Stiernstedt, M., Sundström, A., Adolfsson, R., 2020. Biological and environmental predictors of heterogeneity in neurocognitive ageing: Evidence from Betula and other longitudinal studies.

Ageing Res. Rev. 64. https://doi.org/10.1016/j.arr.2020.101184

Pedersen, R., Geerligs, L., Andersson, M., Gorbach, T., Avelar-Pereira, B., Wåhlin, A., Rieckmann, A., Nyberg, L., Salami, A., 2021. When functional blurring becomes deleterious: Reduced system segregation is associated with less white matter integrity and cognitive decline in aging. Neuroimage 242, 118449. https://doi.org/10.1016/j.neuroimage.2021.118449

Power, J.D., Schlaggar, B.L., Lessov-Schlaggar, C.N., Petersen, S.E., 2013. Evidence for hubs in human functional brain networks. Neuron 79, 798–813. https://doi.org/10.1016/j.neuron.2013.07.035

Rieckmann, A., Hedden, T., Younger, A.P., Sperling, R.A., Johnson, K.A., Buckner, R.L., 2016. Dopamine transporter availability in clinically normal aging is associated with individual differences in white matter integrity. Hum. Brain Mapp. 37, 621–631. https://doi.org/10.1002/hbm.23054

Salami, A., Eriksson, J., Nilsson, L.G., Nyberg, L., 2012. Age-related white matter microstructural differences partly mediate age-related decline in processing speed but not cognition. Biochim. Biophys. Acta - Mol. Basis Dis. 1822, 408–415. https://doi.org/10.1016/j.bbadis.2011.09.001

Salami, A., Rieckmann, A., Karalija, N., Avelar-Pereira, B., Andersson, M., Wåhlin, A., Papenberg, G., Garrett, D.D., Riklund, K., Lövdén, M., Lindenberger, U., Bäckman, L., Nyberg, L., 2018. Neurocognitive Profiles of Older Adults with Working-Memory Dysfunction. Cereb. Cortex 28, 2525–2539. https://doi.org/10.1093/cercor/bhy062

Schilling, K.G., Blaber, J., Hansen, C., Cai, L., Rogers, B., Anderson, A.W., Smith, S., Kanakaraj, P., Rex, T., Resnick, S.M., Shafer, A.T., Cutting, L.E., Woodward, N., Zald, D., Landman, B.A., 2020. Distortion correction of diffusion weighted MRI without reverse phase-encoding scans or field-maps. PLoS One 15, 1–15. https://doi.org/10.1371/journal.pone.0236418

Sexton, C.E., Walhovd, K.B., Storsve, A.B., Tamnes, C.K., Westlye, L.T., Johansen-Berg, H., Fjell, A.M., 2014. Accelerated changes in white matter microstructure during aging: A longitudinal diffusion tensor imaging study. J. Neurosci. 34, 15425–15436. https://doi.org/10.1523/jneurosci.0203-14.2014

Smith, R., Raffelt, D., Tournier, J.-D., Connelly, A., 2020. Quantitative streamlines tractography: methods and inter-subject normalisation 1–27. https://doi.org/10.31219/osf.io/c67kn

Smith, R.E., Tournier, J.D., Calamante, F., Connelly, A., 2015. The effects of SIFT on the reproducibility and biological accuracy of the structural connectome. Neuroimage 104, 253–265. https://doi.org/10.1016/j.neuroimage.2014.10.004

Smith, R.E., Tournier, J.D., Calamante, F., Connelly, A., 2012. Anatomically-constrained tractography: Improved diffusion MRI streamlines tractography through effective use of anatomical information. Neuroimage 62, 1924–1938.

https://doi.org/10.1016/j.neuroimage.2012.06.005

Smith, S.M., 2002. Fast robust automated brain extraction. Hum. Brain Mapp. 17, 143–155. https://doi.org/10.1002/hbm.10062

Smith, S.M., Nichols, T.E., 2009. Threshold-free cluster enhancement: Addressing problems of smoothing, threshold dependence and localisation in cluster inference. Neuroimage 44, 83–98. https://doi.org/10.1016/j.neuroimage.2008.03.061

Sporns, O., Honey, C.J., Kötter, R., 2007. Identification and Classification of Hubs in Brain Networks. PLoS One e1049, 1–14. https://doi.org/10.1371/Citation

Tingley, D., Yamamoto, T., Kentaro Hirose, Keele, L., Imai, K., 2014. mediation: R Package for Causal Mediation Analysis. J. Stat. Softw. 59, 23–38.

Tomasi, D., Wang, G.J., Volkow, N.D., 2013. Energetic cost of brain functional connectivity. Proc. Natl. Acad. Sci. U. S. A. 110, 13642–13647. https://doi.org/10.1073/pnas.1303346110

Tournier, J.D., Smith, R., Raffelt, D., Tabbara, R., Dhollander, T., Pietsch, M., Christiaens, D., Jeurissen, B., Yeh, C.H., Connelly, A., 2019. MRtrix3: A fast, flexible and open software framework for medical image processing and visualisation. Neuroimage. https://doi.org/10.1016/j.neuroimage.2019.116137

Vaishnavi, S.N., Vlassenko, A.G., Rundle, M.M., Snyder, A.Z., Mintun, M.A., Raichle, M.E., 2010. Regional aerobic glycolysis in the human brain. Proc. Natl. Acad. Sci. U. S. A. 107, 17757–17762. https://doi.org/10.1073/pnas.1010459107

van den Heuvel, M.P., de Lange, S.C., Zalesky, A., Seguin, C., Yeo, B.T.T., Schmidt, R., 2017. Proportional thresholding in resting-state fMRI functional connectivity networks and consequences for patient-control connectome studies: Issues and recommendations. Neuroimage 152, 437–449. https://doi.org/10.1016/j.neuroimage.2017.02.005

Van Den Heuvel, M.P., Kahn, R.S., Goñi, J., Sporns, O., 2012. High-cost, high-capacity backbone for global brain communication. Proc. Natl. Acad. Sci. U. S. A. 109, 11372–11377. https://doi.org/10.1073/pnas.1203593109

Van Den Heuvel, M.P., Mandl, R.C.W., Stam, C.J., Kahn, R.S., Hulshoff Pol, H.E., 2010. Aberrant frontal and temporal complex network structure in schizophrenia: A graph theoretical analysis. J. Neurosci. 30, 15915–15926. https://doi.org/10.1523/jneurosci.2874-10.2010

van den Heuvel, M.P., Sporns, O., 2013. Network hubs in the human brain. Trends Cogn. Sci. 17, 683–696. https://doi.org/10.1016/j.tics.2013.09.012

van den Heuvel, M.P., Sporns, O., 2011. Rich-club organization of the human connectome. J. Neurosci. 31, 15775–15786. https://doi.org/10.1523/jneurosci.3539-11.2011

Van Den Heuvel, M.P., Stam, C.J., Kahn, R.S., Hulshoff Pol, H.E., 2009. Efficiency of functional brain networks and intellectual performance. J. Neurosci. 29, 7619–7624.

https://doi.org/10.1523/jneurosci.1443-09.2009

Vinokur, L., Zalesky, A., Raffelt, D., Smith, R.E., Connelly, A., 2015. a Novel Threshold-Free Network-Based Statistical Method: Demonstration and Parameter Optimisation Using in Vivo Simulated Pathology. Ismrm 2874, 297–298.

Wang, H.D., Deutch, A.Y., 2008. Dopamine depletion of the prefrontal cortex induces dendritic spine loss: Reversal by atypical antipsychotic drug treatment. Neuropsychopharmacology 33, 1276–1286. https://doi.org/10.1038/sj.npp.1301521

Waters, G., Caplan, D., 2005. The relationship between age, processing speed, working memory capacity, and language comprehension. Memory 13, 403–413. https://doi.org/10.1080/09658210344000459

Xu, Z., Xia, M., Wang, X., Liao, X., Zhao, T., He, Y., 2022. Meta-connectomic analysis maps consistent, reproducible, and transcriptionally relevant functional connectome hubs in the human brain. Commun. Biol. 5. https://doi.org/10.1038/s42003-022-04028-x

Zalesky, A., Fornito, A., Bullmore, E.T., 2010. Network-based statistic: Identifying differences in brain networks. Neuroimage 53, 1197–1207. https://doi.org/10.1016/j.neuroimage.2010.06.041

Zamani Esfahlani, F., Faskowitz, J., Slack, J., Mišić, B., Betzel, R.F., 2022. Local structure-function relationships in human brain networks across the lifespan. Nat. Commun. 13. https://doi.org/10.1038/s41467-022-29770-y

Zhao, T., Cao, M., Niu, H., Zuo, X.N., Evans, A., He, Y., Dong, Q., Shu, N., 2015. Age-related changes in the topological organization of the white matter structural connectome across the human lifespan. Hum. Brain Mapp. 36, 3777–3792. https://doi.org/10.1002/hbm.22877

Zimmermann, J., Griffiths, J.D., McIntosh, A.R., 2018. Unique mapping of structural and functional connectivity on cognition. J. Neurosci. 38, 9658–9667. https://doi.org/10.1523/jneurosci.0900-18.2018

Zuo, X.N., He, Y., Betzel, R.F., Colcombe, S., Sporns, O., Milham, M.P., 2017. Human Connectomics across the Life Span. Trends Cogn. Sci. https://doi.org/10.1016/j.tics.2016.10.005